Experimental and Molecular Pathology 137 (2024) 104895

Contents lists available at ScienceDirect

Experimental and Molecular Pathology

journal homepage: www.elsevier.com/locate/yexmp

Circulating perturbation of phosphatidylcholine (PC) and phosphatidylethanolamine (PE) is associated to cardiac remodeling and NLRP3 inflammasome in cardiovascular patients with insulin resistance risk

Elena Vianello [a,b,*,1], Federico Ambrogi [c,d,1], Marta Kalousová [e], Julietta Badalyan [f], Elena Dozio [a,b], Lorenza Tacchini [a,b], Gerd Schmitz [g], Tomáš Zima [e], Gregory J. Tsongalis [h], Massimiliano M. Corsi-Romanelli [a,i]

[a] Department of Biomedical Sciences for Health, University of Milan, Milan, Italy
[b] Experimental Laboratory for Research on Organ Damage Biomarkers, IRCCS Istituto Auxologico Italiano, Italy
[c] Department of Clinical Sciences and Community Health, University of Milan, Milan, Italy
[d] IRCCS Policlinico San Donato, San Donato Milanese, Italy
[e] Institute of Medical Biochemistry and Laboratory Diagnostics, First Faculty of Medicine, Charles University and Prague General University Hospital, Prague, Czech Republic
[f] Scuola di Specializzazione in Statistica Sanitaria e Biometria, Università Degli Studi Di Milano, Milan, Italy
[g] Department of Clinical Chemistry and Laboratory Medicine, University Hospital Regensburg, Regensburg, Germany
[h] Dartmouth-Hitchcock Medical Center, Department of Pathology and Laboratory Medicine, Lebanon, NH, USA
[i] Department of Experimental and Clinical Pathology, IRCCS Istituto Auxologico Italiano, Milan, Italy

ARTICLE INFO

Keywords:
Phosphatidylcholine (PC)
Phosphatidylethanolamine (PE)
NOD-like receptor family pyrin domain-containing 3 (NLRP3)
Cardiovascular diseases (CVDs)
Cardiac remodeling
Insulin resistance (IR) risk

ABSTRACT

Lipidome perturbation occurring during meta-inflammation is associated to left ventricle (LV) remodeling though the activation of the NLRP3 inflammasome, a key regulator of chronic inflammation in obesity-related disorders. Little is known about phosphatidylcholine (PC) and phosphatidylethanolamine (PE) as DAMP-induced NLRP3 inflammasome. Our study is aimed to evaluate if a systemic reduction of PC/PE molar ratio can affect NLRP3 plasma levels in cardiovascular disease (CVD) patients with insulin resistance (IR) risk.

Forty patients from IRCCS Policlinico San Donato were enrolled, and their blood samples were drawn before heart surgery. LV geometry measurements were evaluated by echocardiography and clinical data associated to IR risk were collected. PC and PE were quantified by ESI-MS/MS. Circulating NLRP3 was quantified by an ELISA assay.

Our results have shown that CVD patients with IR risk presented systemic lipid impairment of PC and PE species and their ratio in plasma was inversely associated to NLRP3 levels. Interestingly, CVD patients with IR risk presented LV changes directly associated to increased levels of NLRP3 and a decrease in PC/PE ratio in plasma, highlighting the systemic effect of meta-inflammation in cardiac response. In summary, PC and PE can be considered bioactive mediators associated to both the NLRP3 and LV changes in CVD patients with IR risk.

Abbreviations: ADIPO-IR, insulin resistance of adipose tissue; ALT, aspartate aminotransferase; AST, alanine aminotransferase; ATP, adenosine triphosphate; BMI, body mass index; BSA, body surface area; CRP, C reactive protein; CVD, cardiovascular disease; DAMP, damage associated molecular patterns; E/A, ratio between early ventricular filling *E*-wave and atria systole A-wave; EF, ejection fraction; FAME, fatty acid methyl esters; FFA, free fatty acid; HbA1c, glycated hemoglobin; HDL, high-density lipoprotein; HF, heart failure; HOMA-IR, homeostatic model of insulin resistance; IL, interleukin; IR, insulin resistance; LA, left atrium; LV, left ventricle; LVM, left ventricle mass; NLRP3, NOD-like receptor family pyrin domain-containing 3; PC, phosphatidylcholine; PE, phosphatidylethanolamine; ROS, reactive oxygen species; RTW, relative wall thickness; TGF-β, tissue growth factor; WHR, waist hip ratio.

* Corresponding author at: Department of Biomedical Sciences for Health, Università degli Studi di Milano "LA STATALE", via Mangiagalli 31, 20133 Milan, Italy.
E-mail address: elena.vianello@unimi.it (E. Vianello).

[1] These authors contributed equally to this work.

https://doi.org/10.1016/j.yexmp.2024.104895
Received 5 December 2023; Received in revised form 25 March 2024; Accepted 12 April 2024
Available online 3 May 2024

1. Introduction

Lipid species derived from cells, tissue, and whole body fluids form the human lipidome(Hornemann, 2022). Lipids have multiple biological functions including the maintenance of cell architecture, energy storage and cell signaling (van Meer, 2005). Moreover, it is well recognized that an impaired lipidome is implicated in several disorders such as degenerative injuries like Alzheimer's disease and multiple sclerosis, and in metabolic disorders, including diabetes and obesity (Agarwal and Khan, 2020; Bergland et al., 2020; Kao et al., 2020; Quintana et al., 2012; Xie et al., 2022; Kane et al., 2021; Jaiswal et al., 2014; Engin, 2017a; Engin, 2017b). Different studies have highlighted the health risks associated to adverse lipid profile analyzing the rough lipid phenotype as total triglycerides or cholesterol in dyslipidemia-associated disorders (Fernandez et al., 2013). Indeed, an impaired adipose tissue lipolysis is a common metabolic reprogramming present both in obesity and cardiovascular diseases (CVD) and it is firstly characterized by a glycolytic switch as a consequence of chronic adrenergic stimulation (Guilherme et al., 2023). This lipidic impairment leads to systemic metabolic disturbances, such as glucose intolerance and insulin resistance, with elevated plasma levels of free fatty acid (FFA) and circulating bioactive metabolites, known as lipokines, derived from local and systemic lipid turnover (Murakami, 2011). Different emerging lipokines are identified as main players to the harmful effect of obesity related cardiovascular disorders (D'Souza et al., 2016; Wasserman et al., 2020; Wallace et al., 2014; Gong et al., 2011; Scheja and Heeren, 2019). Among these, phosphatidylcholine (PC) and phosphatidylethanolamine (PE) have gained attention from the 1950s thanks to Eugene Kennedy and coworkers who highlighted the impact of phospholipid metabolism on health and diseases, suggesting the use of an abnormal PC/PE molar ratio as a biomarker of disease progression, in liver, intestine and skeletal muscle, during obesity-related disorders (Kennedy, 1957; van der Veen et al., 2017). Indeed, systemic PC/PE content is firstly affected by a high fat diet that initiates enhanced cellular choline uptake and promotes abnormal phospholipid turnover in the tissue (Kumar et al., 2021; van der Veen et al., 2017). Moreover, an increased choline uptake, which occurs in inflammatory sites such as tumors, inflamed joints, and atherosclerotic plaques, is necessary to enhance cancer cell proliferation or inflammatory cell commitment (Laitinen et al., 2010; Hellberg et al., 2016; Roppongi et al., 2019; Seki et al., 2017). One of the essential conditions to activate macrophages in the pro-inflammatory M1 phenotype, is the uptake of choline at inflamed sites, to carry out macrophages-mediated interleukin (IL)-1β dependent inflammation (Sanchez-Lopez et al., 2019). The newly uptaken choline is rapidly converted to PC as a sign of energy cost of inflammatory cytokine production by resident cells (Snider et al., 2018; Sanchez-Lopez et al., 2019; Frostegard, 2022; van der Veen et al., 2017). This increase in the lipolytic rate is also reported in heart failure where perturbations in the cardiac lipidome decreases the PC/PE ratio with accompanied cell damage due to the loss of membrane integrity (Warmbrunn et al., 2021; Agarwal and Khan, 2020; Carvalho et al., 2022). PC and PE regulated cell membrane fluidity and stability and the reduction of PC/PE ratio is directly related to the left ventricle decline in adipose tissue specific adipose triglyceride lipase deficient mice (Salatzki et al., 2018). This is because lipids play a central role in CVD development, and they are traditional predictors of cardiovascular events (Rivas Serna et al., 2021; Warmbrunn et al., 2021; Fernandez et al., 2013; Michos et al., 2019; Liu et al., 2022) but the molecular mechanisms governing cardiac inflammation depending on PC and PE systemic content are largely unknown. One study highlighted that the NOD-like receptor family pyrin domain-containing 3 (NLRP3) is the potential missing link between meta-inflammation (i.e. metabolically-induced inflammation) (Li et al., 2020; Suceveanu et al., 2020) and cardiovascular outcome (Sokolova et al., 2020; Kelley et al., 2019). NLRP3, a member of Nod-like receptor (NLR) family, is a multiproteic inflammatory platform which responds to numerous stimuli such as reactive oxygen species (ROS)(Dominic et al., 2022), cholesterol crystal (Grebe et al., 2018), and extracellular adenosine triphosphate (ATP)(Higashikuni et al., 2023), recognizing them as damage associated molecular patterns (DAMP) and triggers inflammation through IL-1β and IL-18 production and secretion by competent cells (Zhan et al., 2022). Among DAMP-induced NLRP3, emerging bioactive lipids like sphingolipids and ceramides are identified as first players of meta-inflammation sustained by NLRP3 inflammasome (Li et al., 2020; Suceveanu et al., 2020). These findings have shown also that the exposure to circulating lipidic DAMPs as ceramides and phospholipids, can further lead to activation of caspase-1, pro-inflammatory cytokines release, including collagen and tissue growth factor (TGF)-β, and tissue injury and fibrosis (Qiu et al., 2019; Vandanmagsar et al., 2011; Mridha et al., 2017). Due to the lack of studies focused on lipidomic impairment and cardiac remodeling, the objective of the present study is to verify in an overweight CVD population how the insulin resistance risk can affect systemic PC/PE molar content and promote left ventricle (LV) morphological changes through the NLRP3 inflammasome.

2. Materials and methods

2.1. Study population

This study enrolled 40 overweight CVD male patients at the IRCCS Policlinico San Donato (San Donato Milanese, Milan, Italy) scheduled for open heart surgery: thirty patients with three vessel disease underwent bypass graft surgery and ten patients underwent valve replacement due to aortic stenosis. The overweight is evaluated using body mass index (BMI) ranged between 25 to 29.9 (Obesity: preventing and managing the global epidemic. Report of a WHO consultation, 2000). Patients with recent acute myocardial infarction, malignant disease, prior major abdominal surgery, renal failure, end-stage heart failure (HF) and more than 3% change in body weight in the previous three months were excluded. Demographic, anthropometric, and clinical data including age, sex, and family history of hypertension, diabetes and coronary artery disease were recorded. Before surgery, left ventricle (LV) measurements were quantified by echocardiography and diastolic function was evaluated by left atrium (LA) measurement and eco doppler.

2.2. Blood collection and measurements

3 ml of blood sample was collected after overnight fasting into pyrogen-free tubes with ethylenediaminetetraacetic acid as anticoagulant. Plasma samples were separated after centrifugation at 1000 g for 15 min and were stored at -20°C until analysis. The following parameters were measured as part of standard medical examinations: fasting glucose (mg/dl), fasting insulin (microU/ml), total cholesterol (mg/dl), triglycerides (mg/dl), glycated hemoglobin (HbA1c; %), creatinine (mg/dl), C-reactive protein (CRP; mg/dl), uric acid (md/dl), alanine aminotransferase (AST) (U/l), aspartate aminotransferase (ALT) (U/l), total bilirubin and protein were quantified with commercial kits using a Cobas 6000 analyzer (Roche Diagnostics, Milan, Italy). NLRP3 in plasma were measured by enzyme-linked immunosorbent assay (ELISA) (MyBioSource, San Diego, California, USA).

2.3. Insulin resistance risk assessment using HOMA-IR and ADIPO-IR

The insulin resistance (IR) risk was assessed by the homeostatic model of insulin resistance (HOMA-IR) and ADIPO-IR, the two indexes used to estimate glucose and insulin tolerance in the body (Sondergaard et al., 2017; Shalaurova et al., 2014). HOMA-IR estimates insulin sensitivity and beta-cell function reflecting hepatic IR and glucose metabolism. HOMA-IR was calculated using this formula:

$$\mathrm{HOMA-IR} = \text{fasting glucose x fasting insulin}/22.5$$

HOMA-IR cut off values in adults without IR ranged between 0.23-

2.5. Value greater than 2.5 indicates possible IR complications and glucose intolerance.

ADIPO-IR is an early marker of IR and measures the resistance to antilipolytic effect of the insulin in adipose tissue and it was calculated as follows:

$$\text{ADIPO} - \text{IR} = \text{free fatty acid (FFA) x fasting insulin}$$

There is not a recognized cut off value for ADIPO-IR but it increases progressively across the span of adiposity from normal weight to overweight/obese. The higher ADIPO-IR the worse the lipid profile.

2.4. Echocardiography data of left ventricular mass (LV) end pulsed-wave doppler

Pre-surgical resting echocardiography (Vingmed-System Five; General Electric, Horten, Norway) was done to examine systolic, diastolic, and valvular morphology and function. LV morphology and function was defined according to current guidelines for echocardiographic chamber quantification(Lang et al., 2015). LV diastolic diameter, LV diastolic diameter/height, LV diastolic volume, LV systolic volume, LV diastolic volume/body surface area (BSA) measures were taken to assess LV dimension and volume (Table 1). To estimate LV mass enlargement, relative wall thickness (RTW) was calculated by linear mode, while LV mass (LVM) and indexed LV mass (h LVM) were measured by 2-D mode. The LV systolic function was evaluated using ejection fraction (EF) by the 2-D mode method. Diastolic function is evaluated using pulsed-wave doppler in the apical four-chamber view to obtain mitral flow velocities to assess LV filling. Measurement of mitral flow included the peak early filling (E-wave) and late diastolic filling (A-wave) velocities, and the E/A of early filling velocity. All data and reference values are reported in Table 1. Clinical evaluation of LV geometry and filling were assessed and referenced according to recommendations for cardiac chamber quantification by echocardiography from the American Society of Echocardiography and the European Association of Cardiovascular Imaging (Lang et al., 2015; Baumgartner et al., 2017).

2.5. Free fatty acid analysis by gas chromatography/mass spectrometry (GC–MS)

Free fatty acid (FA) analysis was a performed on fatty acid methyl esters (FAME) generated with acetyl-chloride and methanol and extracted with hexane. Total FA analysis was carried out using a Shimadzu 2010 GC-MS system. FAME were separated by a BPX70 column (10 m length, 0.10 mm diameter, 0.20 μm film thickness) from SGE using helium as carrier gas. The initial oven temperature was 50°C which was programmed to increase at a rate of 40°C per min to 155°C, with 6°C per min to 210°C, and with 15°C per min to finally reach 250°C. The FA species and their positional and *cis/trans* isomers were characterized in scan mode and quantified by single-ion monitoring mode detecting the specific fragments of saturated and unsaturated FAs (saturated: *m/z* 74; monounsaturated: *m/z* 55; diunsaturated: *m/z* 67; polyunsaturated: *m/z* 79). As an internal standard, non-naturally occurring C13:0 was used.

2.6. Lipid analysis by electrospray ionization tandem mass spectrometry (ESI-MS/MS)

Total lipid extraction and purification was performed according to the protocol described by Blight and Dyer(Bligh and Dyer, 1959). Lipid species were quantified by ESI-MS/MS using methods validated and described previously(Wiesner et al., 2009). In brief, starting from plasma, samples were analysed by direct flow injection on a Quattro Ultima triple-quadrupole mass spectrometer (Micromass, Manchester, UK) using a HTS PAL autosampler (Zwingen, Switzerland) and an Agilent 1100 binary pump (Waldbronn, Germany) with a solvent mixture of methanol containing 10 mM ammonium acetate and chloroform (3:1, v/

Table 1
Clinical characteristics and echocardiographic assessment of overweight CVD patients.

Variable	Mean	Std. Dev.	Normality	Age matched male reference values
Age (years)	64,44	9,27	no	na
BSA (m^2)	1,89	0,17	no	na
BMI	**27,55**	3,06	no	18,50-24,90
Weight (Kg)	79,85	11,80	no	na
Height (m)	1,70	0,08	no	na
Waist (cm)	**103,50**	9,33	no	<94,00-102,00
Hip (cm)	102,90	8,69	no	na
WHR	**1,01**	0,09	no	0,94
Fasting glucose (mg/dl)	94,29	37,82	no	70,00-100,00
Fasting insulin (mlU/ml)	8,77	5,26	no	2,00-20,00
NLRP3 (ng/ml)	1,61	0,54	no	na
HOMA-IR	2,08	1,69	no	0,40-2,40
ADIPO-IR	69,28	59,63	no	na
Total cholesterol (mg/dl)	**159,40**	45,59	no	<150,00
HDL (mg/dl)	36,76	8,29	no	<50,00
Triglyceride (mg/dl)	144,60	78,13	no	<150,00
Acid uric (mg/dl)	5,86	1,14	no	3,50-7,20
Creatinine (mg/dl)	1,05	0,40	no	0,74-1,35
CRP (mg/dl)	0,81	2,10	no	<10,00
Systolic blood pressure (mmHg)	**121,10**	9,50	no	120,00
Diastolic blood pressure (mmHg)	71,11	4,65	no	80,00
ALT (U/l)	33,37	25,63	no	4,00-36,00
AST (U/l)	26,22	15,57	no	8,00-33,00
Bilirubin (total) (mg/dl)	0,67	0,32	no	0,10-1,20
HbA1c (%)	5,86	1,16	yes	<6,00
Total protein (g/L)	6,49	0,32	no	60,00-83,00
LV dimension				
LV diastolic diamenter (cm)	5221	0,85	yes	4,20-5,90
LV diastolic diamenter/BSA (cm/m^2)	59,23	23,90	no	2,20-3,10
LV diastolic diameter/height (cm/m)	3088	0,45	no	2,40-3,30
LV volume				
LV diastolic volume (ml)	113,90	53,59	no	22,00-58,00
LV systolic volume (ml)	49,93	34,03	no	22,00-58,00
LV diastolic volume/BSA (ml/m^2)	59,23	23,90	no	35,00-75,00
LV systolic volume/BSA (ml/m^2)	25,75	15,91	no	12,00-30,00
LV mass				
Relative wall thickness (RTW) (%)	**0,45**	0,10	no	<0,42
LVM (g)	**256,70**	109,80	no	96,00–200,00
LVM indexed (%)	**134,50**	50,71	no	50,00-102,00
LV systolic function				
Ejection fraction (%)	59,35	11,59	no	≥55,00
Diastolic function				59 ± 13
Left atrium (LA) (cm)	**4,48**	0,78	no	3,00-4,00
E/A	**0,97**	0,47	no	≥1

Clinical data, body fatness measurements and echocardiographic assessment are shown in Table 1. The CVD population had higher indexes of body fatness and abnormal values for total cholesterol, BMI, waist circumference and WHR, indicating that CVD patients were overweight as reported by L.F.J. Visseren et al

in the ESC Guidelines on cardiovascular disease prevention in clinical practice (Visseren et al., 2022). Echocardiographic data show that the overweight CVD population is chacterized by left ventricle (LV) dilation with a preserved ejection fraction (EF%) suggeting an proportional expansion of plasma volume with their body mass.

The overweight CVD population affected by chronic overload presented LV remodeling and compromised early ventricular filling volume and apical untwist expressed as E/A<1 and LA> 4cm, following the guidelines for cardiac chamber quantification by echocardiography revised in 2015 (Lang et al., 2015).

The normality distribution is assessed using D'Agostino & Pearson omnibus normality test.

Abbreviations: BSA, body surface area; BMI, body mass index; WHR, waist hip ratio; NLRP3, NOD-like receptor family pyrin domain-containing 3; HOMA-IR, homeostatic model of insulin resistance; ADIPO-IR, insulin resistance of adipose tissue; HDL, High-Density Lipoprotein; CRP, C reactive protein; AST, alanine aminotransferase; ALT, aspartate aminotransferase; HbA1c, grycated hemoglobin; LA, left atrium; LV left ventricle; RTW, relaltive wall thickness; LVM, left ventricle mass; E/A, ratio between early ventricular filling *E*-wave and atria systole A-wave; EF, ejection fraction; na, not applicable.

v). A flow gradient was performed starting with a flow of 55 μl/min for 6 seconds followed by 30 μl/min for 1.0 min and an increase to 250 μl/min for another 12 seconds. A precursor ion scan of m/z 184 specific for phosphocholine containing lipids was used for phosphatidylcholine *(PC)*. A neutral loss scan of m/z 141 was used for phosphatidylethanolamine (PE). Quantification was achieved by calibration lines generated by addition of naturally occurring lipid species (extraction of 20μl 5-fold diluted plasma for single FPLC fractions or 20μl undiluted plasma for pooled lipoprotein fractions). All lipid classes were quantified with internal standards belonging to the same lipid class. Calibration curves were generated for the following naturally occurring species: PC 34:1, 36:2, 38:4, 40:0, and PC O 16:0/20:4; and PE p16:0/20:4. These calibration curves were also applied for non-calibrated species, as follows: concentrations of saturated, monounsaturated, and polyunsaturated species were calculated using the closest related saturated, monounsaturated, and polyunsaturated calibration curve slope, respectively. For example, PE 36:2 calibration was used for PE 36:1, PE 36:3, and PE 36:4; PE 38:4 calibration was used for PE 38:3, PE 38:5, etc. Ether-PC species were calibrated using PC O 16:0/20:4 and PE-pl were quantified independently from the length of the ether linked alkyl chain using PE p16:0/20:4. From this analysis the PC/PE ratio was calculated as total sum.

2.7. Statistical analysis

Comparison between groups was performed using two-tailed unpaired Student t test or Mann-Whitney U-test as appropriate (GraphPad Prism 9). Spearman or Pearson correlation analysis were used to examine association among different variables. Partial Least Squares Discriminant Analysis (PLS_DA) (Le Cao et al., 2011) and Correlogram were performed using the mixOmics R package (Rohart et al., 2017). PLS-DA was useful as a dimensional reduction technique in classification problems. The classification variable was represented by HOMA < 2.5 or NLRP3 with median as cutoff, while the explanatory variables were PC, PE, and PC/PE ratio in plasma.

3. Results

3.1.1. Clinical and echocardiographic characteristics of CVD patients enrolled in the study

All the clinical characteristics as mean and standard deviation (Std. Dev.), and their age matched reference values of overweight CVD men are reported in Table 1. The overweight CVD population presented a cardiometabolic profile associated to the risk of second event of CVD complications. The overall characteristics of CVD patients are associated to insulin resistance risk (BMI:27.5; Waist:103.50cm; WHR:>102; total cholesterol:>150.00 mg/dl; systolic blood pressure>120 mmHg); LV enlargement (RTW:>0.42%; LV masses: >200.00g LVM and >102.00% LVM indexed), and diastolic dysfunction (LA>4cm, altered E/A); the main co-factors responsible to the onset and progression of heart failure (HF), the end stage of CVD complications. All the anthropometric parameters refer to the ESC Guidelines on cardiovascular disease in clinical practice.(Visseren et al., 2022).

3.1.2. Differential expression of PC and PE in plasma according to IR indices in CVD overweight patients

We performed targeted PC and PE metabolite testing in plasma using electrospray ionization tandem mass spectrometry (ESI-MS/MS).

To better understand how insulin resistance risk can influence PC and PE profiles, we stratified CVD patients according to HOMA-IR (<2.5 and ≥2.5) and ADIPO-IR. Ten top differential expressions of PC in plasma are represented in the heatmap (Fig. 1a). CVD patients with HOMA-IR <2.5 (green color named "0" in the legend) are associated to different lipidic PC and PE profiles than CVD patients with HOMA≥2,5 (red color named "1" in the legend) (Fig. 1a). Differences are shown in PC_36:4 ($p<0.001$); PC_34_1 ($p<0.05$); PC_O_40:6($p<0.05$); PC_38:4; PC_34:2; PC_38:5; PC_36:3; PC_32:1 and PC_34:3 (ADIPO-IR classification is not shown). Correlograms among all PC circulating species and HOMA-IR and ADIPO-IR are reported in Fig. 1b and c. Increasing HOMA-IR (Fig. 1b) and ADIPO-IR (Fig. 1c) significantly affected all annotated PC in plasma (Fig. 1b).

Regarding PE in plasma, the 10 top differential expressions of them are represented in Fig. 2a. The heatmap shows that CVD patients with HOMA-IR <2.5 are associated with a unique PE presence than patients with HOMA≥2.5 (Fig. 2a). These differences including PE_36:1 ($p<0.001$); PE_38:4 ($p<0.001$); PE_32:0 ($p<0.05$); PE_36:4 ($p<0.05$); PE_34:1($p<0.05$); PE_38:5 ($p<0.05$); PE_40:6($p<0.05$); PE_38:6 ($p<0.05$); PE_36:2 8p=0.05); PE_40:4 ($p=0.07$). Correlograms among PE in plasma and HOMA-IR (Fig. 2b) and ADIPO-IR (Fig. 2c) highlight the correlations among PE species and IR indexes, showing how being overweight can promote PE abnormalities in the bloodstream.

3.1.3. Association between insulin resistance risk, PC and PE profile, and NLRP3 circulating levels

PC and PE profile were globally compared using Partial Least Square Discrimination Analysis (PLS-DA), a categorization method which optimized the classification among the different groups of samples. To categorize our population, we used HOMA-IR and not ADIPO-IR because this index represents the whole IR body risk. The 10 top differential expressions of PC and PE in plasma are globally represented in Fig. 3. Using 3-fold cross validation 2 components with 46 and 8 features were used in PLS-DA classification (Fig. 3a). According to component 1 with HOMA-IR≥2.5 (Fig. 3b), PC and PE selected variables show a different distribution compared to PC and PE variables according to component 2 with HOMA-IR<2.5 (Fig. 3c). The color of each variable corresponds to the group where the mean is maximum. For example, PC_40:5 has mean value grater in class 0 (HOMA< 2.5) than 1. These graphs highlight how the IR risk can influence the PC and PE lipid profile in plasma with a reduction of the main species (Fig. 3b) than in CVD patients without IR risk (Fig. 3c). The selected variables are used to create a heatmap (Fig. 3d). On the left side of the heatmap each row is labeled with 0 (HOMA-IR< 2.5) or 1 (HOMA-IR ≥ 2.5). On the right side NLRP3 is represented categorized in quartiles: green is the lowest quartile, blue is the second quartile, orange the third quartile and red the fourth quartile. The heatmap reveals that several PC and PE species are related to the increase of both HOMA-IR and NLRP3 circulating levels.

3.1.4. PC and PE categorization using NLRP3 median cut-off

To evaluate NLRP3 association with plasma PC and PE in CVD patients with IR risk, we performed a PLS-DA method, categorizing lipid

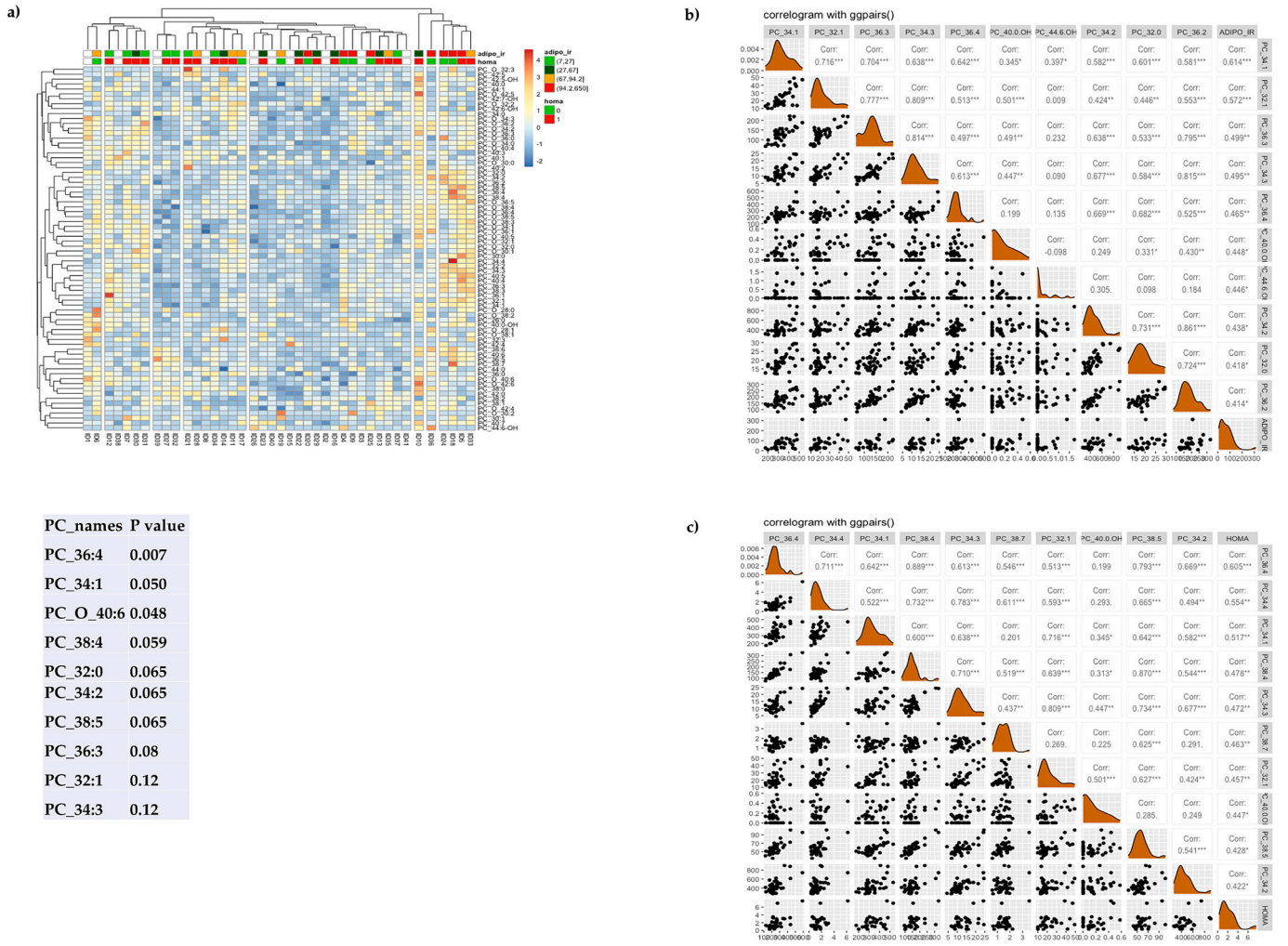

PC_names	P value
PC_36:4	0.007
PC_34:1	0.050
PC_O_40:6	0.048
PC_38:4	0.059
PC_32:0	0.065
PC_34:2	0.065
PC_38:5	0.065
PC_36:3	0.08
PC_32:1	0.12
PC_34:3	0.12

Fig. 1. Differential expression of PC in plasma of CVD patients influenced by insulin resistance (IR) risk.
The differential expressions of PC in plasma of CVD patients stratified according to HOMA and ADIPO-IR. a) 10 top differential expressions of PC in plasma are represented in the heatmap. The figure shows the PC plasma quantity influenced by IR risk.
CVD patients with IR risk (HOMA≥2.5 named 1 on the legend and high value of ADIPO-IR, both in red color) have a distinct PC profile from CVD patients without IR risk (HOMA<2.5 named 0 and low ADIPO-IR value marked both with green color). They differ in PC_36:4; PC_34:1; PC_O_40:6; PC_38:4; PC_34:2; PC_38:5; PC_36:3; PC_32:1 highlighting that IR risk can influence PC species at systemic level although weakly statistically significant in most metabolites. The correlograms represented in b and c show the positive association between PC metabolites in CVD plasma samples and IR risk indexes, highlighting the statistically significative correlations among PC plasma level and both ADIPO-IR (b) and HOMA (c) increase.

species according to the NLRP3 median cut-off of 1.48ng/ml (Fig. 4a). 3-fold cross validation 2 components with 39 and 1 features were used in PLS-DA classification. PC and PE species are differentially represented in plasma of CVD patients with low or high level of NLRP3 (Fig. 4b and c). The selected variables are used to make a heatmap according to the NLRP3 median cut-off (Fig. 4d). PC and PE in plasma are significantly decreased in CVD patients with IR risk and NLRP3 increased levels.

3.1.5. PC/PE molar ratio in plasma is negatively associated to NLRP3 level and LV relative wall thickness

PC and PE content alteration is implicated in metabolic disorders such as IR, obesity, and atherosclerosis. Decreased PC/PE molar ratios have negative impact on metabolism of different tissues including heart. In our study, CVD patients with IR risk (HOMA≥2.5) showed increased NLRP3 plasma levels (Fig. 5a) and lower plasma PC/PE molar ratios (Fig. 5b) than CVD patients without IR risk (HOMA<2.5); the same results were observed categorizing CVD patients according to ADIPO-IR (data not shown). Moreover, the overall CVD overweight population presented a negative association between PC/PE molar ratio and NLRP3 circulating level in plasma (Spearman r=-0.70 p<0,0001) (Fig. 5c).

3.1.6. PC/PE molar ratio and NLRP3 in plasma are associated to cardiac modification in overweight CVDs patients with IR risk

To better understand the association of our variables and heart maladaptation in presence of IR risk, we divided our cohort according to HOMA cut off. Sixteen overweight CVD patients without IR risk, expressed as HOMA less than 2.5, did not exhibit statistically significant associations between both NLRP3 and PC/PE, and the cardiac parameters of LV remodeling and diastolic function (data not shown). In contrast, twenty-four overweight CVD patients with HOMA≥2.5, showed a strong association between heart remodeling indexes and both PC/PE and NLRP3 variables (Fig. 6). NLRP3 independent variable showed a positive association between diastolic blood pressure (Sperman R= 0.57; p<0.03); end diastolic diameter (Sperman R=0.29; p<0.01), relative wall thickness (Sperman R=0.43; p<0.04) and LV diastolic volume/BSA (Sperman R=0.55; p<0.01), suggesting its molecular involvement in inflammation-induced maladaptive cardiac responses (Fig. 6a). Regarding diastolic disfunction, using LA parameter, we observed that overweight CVD patients with IR risk and larger LA (>4cm) presented higher NLRP3 plasma level than patients with normal LA (<4 cm) (1.59±0.45 ng/ml than 1.09±0.53 ng/ml respectively)

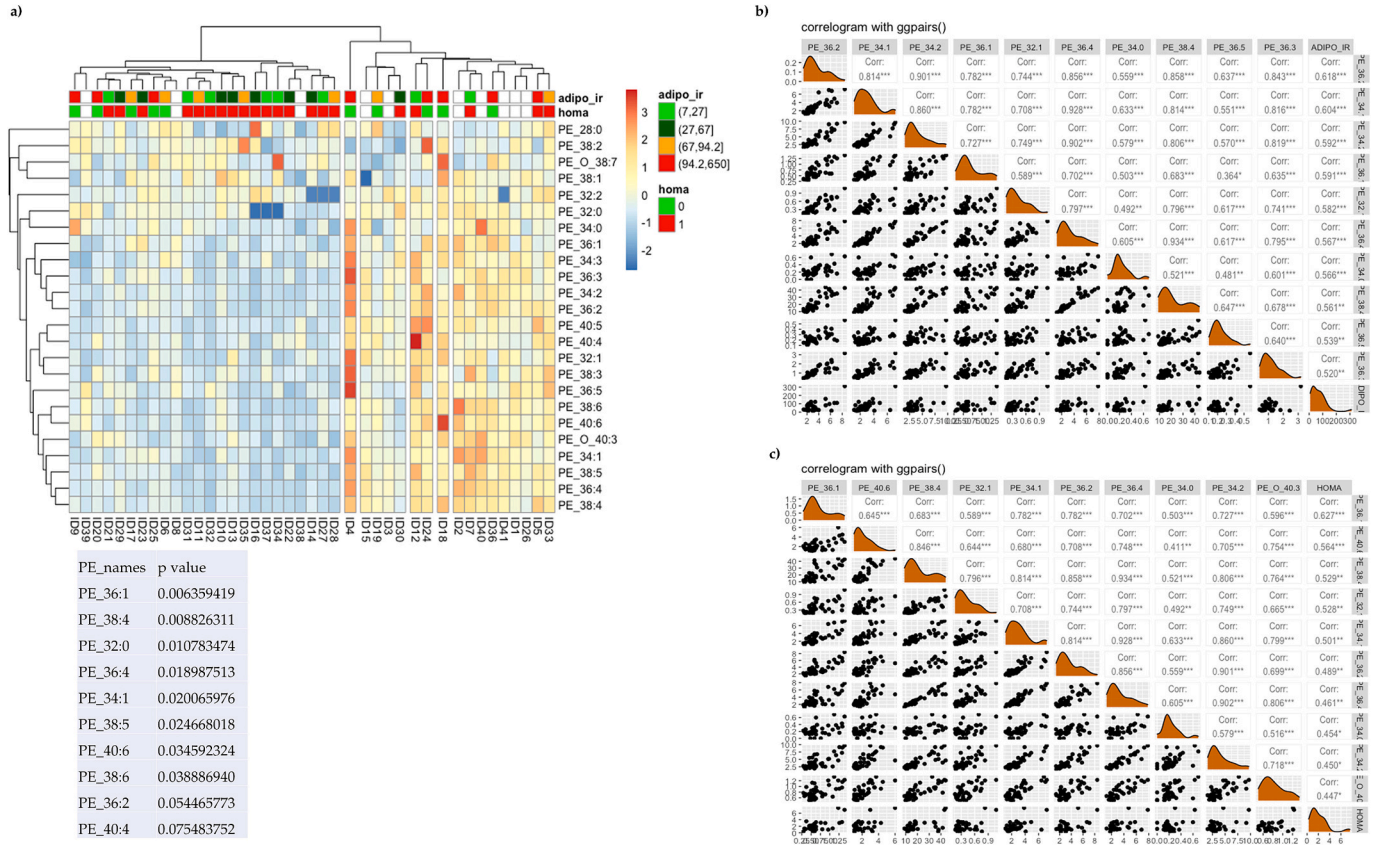

PE_names	p value
PE_36:1	0.006359419
PE_38:4	0.008826311
PE_32:0	0.010783474
PE_36:4	0.018987513
PE_34:1	0.020065976
PE_38:5	0.024668018
PE_40:6	0.034592324
PE_38:6	0.038886940
PE_36:2	0.054465773
PE_40:4	0.075483752

Fig. 2. Differential expression of PE in plasma of CVD patients influenced by insulin resistance (IR) risk.
The differential expressions of PE in plasma of CVDs patients stratified according to HOMA and ADIPO-IR. a) 10 top differential expressions of PE in plasma are represented in the heatmap. The figure shows the PE plasma quantity influenced by IR risk, using both HOMA and ADIPO-IR.
CVD patients with IR risk (HOMA≥2.5 named 1 on the legend and high value of ADIPO-IR, both in red color) have a distinct PE profile from CVD patients without IR risk (HOMA<2.5 named 0 and low ADIPO-IR value marked both with green color). They statistically differ in PE_36:1; PE_38:4; PE_32:0; PE_36:4; PE_34:1; PE_38:5; PE_40:6; PE_38:6; PE_36:2; PE_40:4 highlighting that IR risk can influence PE species at systemic level. The correlograms represented in b and c show the positive association between PE metabolites in CVD plasma samples and IR risk indexes, highlighting the statistically significative correlations among PE plasma level and both ADIPO-IR (b) and HOMA (c) increase.

(Fig. 6b), suggesting a potential involvement of NLRP3 inflammasome and LA filling, one of the first step leading to HF. No statistically differences are observed in PC/PE levels according to LA measurement.

4. Discussion

In the present study we investigated the influence of meta-inflammation on heart morphology in overweight CVD population, highlighting the possible involvement of PC and PE systemic impairment as DAMP-induced NLRP3 inflammasome. Meta-inflammation is a typical trait of individuals who are overweight, characterized by a metabolic switch on glycolysis and FFA systemic release. The progressive dyslipidemia linked to poor fasting blood glucose level, contributes to systemic lipidomic in balance as a predictor of pre-diabetic or diabetic state and adverse cardiovascular outcomes (Rivas Serna et al., 2021). This study showed that overweight CVD patients presented with the two main metabolic traits associated with the development of secondary cardiovascular events promoted by an initial IR stage. Indeed, they presented both anthropometric and metabolic signatures accepted by scientific and clinical communities to diagnose early IR, like common anthropometric parameters (i.e. BMI, waist and WHR measurements) which reflected abdominal fat tissue deposition, and early markers of glucose intolerance, as HOMA-IR and ADIPO-IR, which reveal the resistance of the antilipolytic effect of insulin in liver and adipose tissue respectively (Shalaurova et al., 2014; Sondergaard et al., 2017; Gaggini et al., 2019). To better understand the IR influence on lipid species impairment, we stratified our CVD population according to an earlier index of IR onset, using HOMA-IR and ADIPO-IR. IR risk implied systemic lipid turnover as a consequence of FFA overflow in liver, heart and adipose tissue. In our CVD patients with IR risk, the lipid profile shifts to peculiar phospholipid turnover, with different abundancy of PC and PE systemic content than CVD patients without IR risk. This discrepancy can be explained given that at inflamed sites, like atherosclerotic plaques, the uptake of choline, the essential human nutrient serving a precursor of membrane phospholipids, is also used as a substrate to synthetize new cells and pro-inflammatory chemokines, as well as PC and PE bioactive metabolites, to counteract extending inflammation (Sanchez-Lopez et al., 2019). Indeed, plasma bioactive lipid mediators can act as DAMP and activate NLRP3 immune responses in obesity-related disorders, including myocardial failure(Sokolova et al., 2020). The NLRP3 inflammasome is a multiproteic box able to induce caspase-1 and subsequently IL-1β and IL-18 release in response to DAMP presence at inflamed site. Using Partial Least Squares Discriminant Analysis approach, we observed that CVD patients with IR risk have an overall reduction of plasma PC-related metabolites when NLRP3 levels increased, suggesting the strong impact of meta-inflammation-mediated lipid impairment. Indeed, meta-inflammation alters bioactive lipid mediators into the bloodstream, which function as DAMP and activate immune responses driven by NLRP3 inflammasome. It was recently demonstrated that NLRP3 is induced by higher level of ceramides in myocardial remodeling in an obese rat model (Chaurasia et al., 2021; Rayner et al., 2018; Chaurasia and Summers, 2018, 2021). In our study,

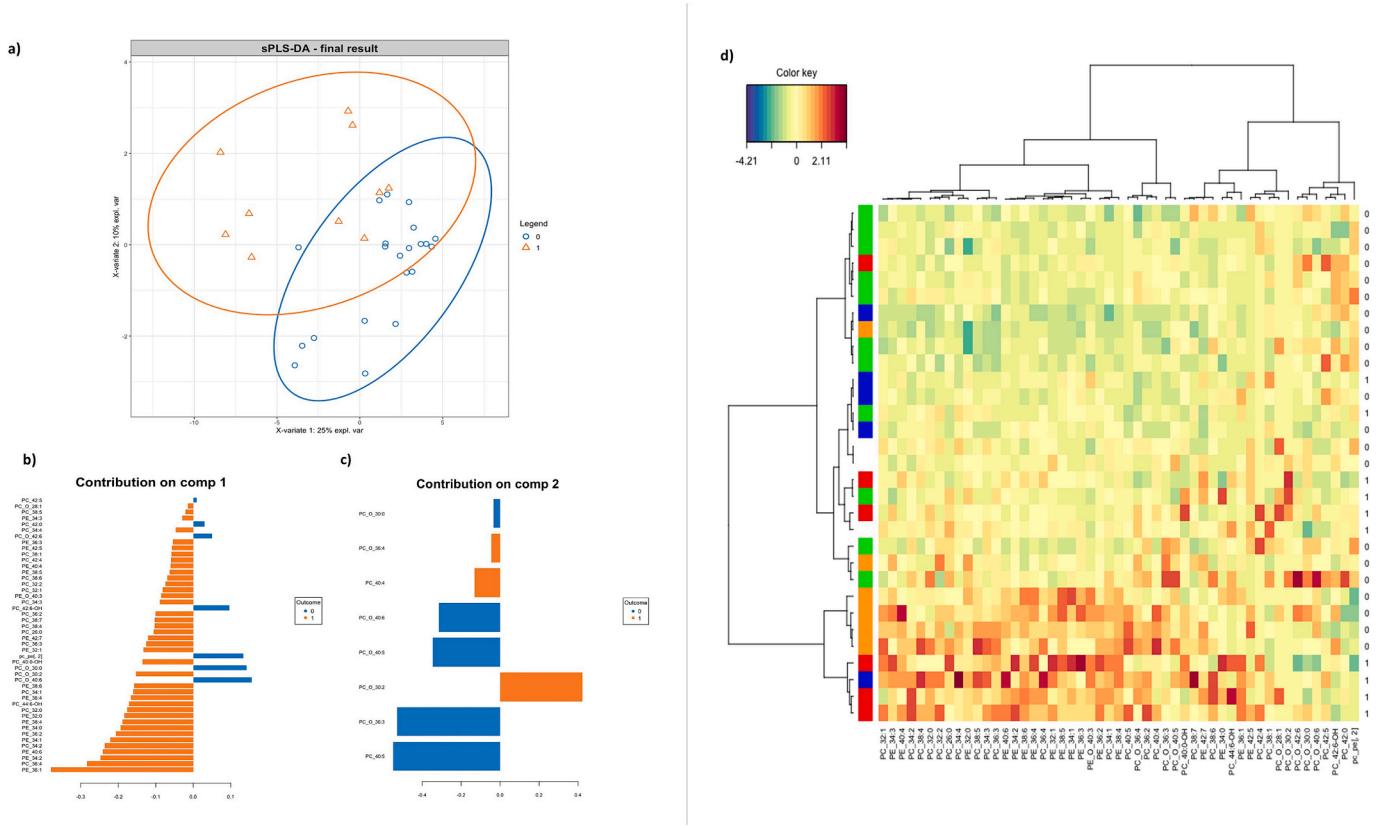

Fig. 3. PLS-DA categorization of PC and PE plasma species in CVD patients according to IR-risk. a) Scores plot of first two PLS components obtained by Partial Least Squares-Discriminant Analysis (PLS-DA). Lipid profile of PC and PE were globally compared using PLS-DA analysis which shows that overweight CVDs patients with (1) or without IR risk (0) are separated. Using 3-fold cross validation 2 components with 46 and 8 features were used in PLS-DA classification. b) According to component 1, most of PC and PE species are reduced in presence of IR risk (HOMA≥2,5; outcome 1) than its absence (HOMA<2,5; outcome = 0) (c). The selected variables are used to create an heatmap (d). On the right side NLRP3 is represented categorized in quartiles: green is the lowest quartile, blue is the second quartile, orange the third quartile and red the fourth quartile. The heatmap reveals how PC end PE species are distributed in the plasma of overweight CVD patients with or without IR risk in presence of low or high NLRP3 plasma level (right side). (For interpretation of the references to color in this figure legend, the reader is referred to the web version of this article.)

NLRP3 seems to respond to lipotoxicity increasing its level in CVD patients who present IR risk and low level of PC circulating species. In contrast, PE plasma level is higher in CVD patients presenting with both IR risk and NLRP3 increased level (fourth quartile of NLRP3 plasma values). In particular they have increased circulating levels of PE 32:1, PE 34:1, PE 34:2, PE 36:2, PE 36:3, PE 38:4, PE 38:5, PE 38:6, PE 40:4, PE 40:6, PE_O 40:6. For this reason, we can suggest that circulating bioactive PE can be the potential DAMP-induced NLRP3 inflammasome in CVD patients with IR risk. The PC bioactive metabolites seem to reduce their level when NLRP3 inflammasome is over expressed. These results are in line with other studies which demonstrated that a lower level of PC individual species is a potential marker of poor cardiovascular health (Rivas Serna et al., 2021). In particular, they reported that the pressure-induced cardiac failure can accompany marked changes in the cardiac lipidome identifying PE38:6 as most PE blood pressure markers, susceptible to pressure variation, and obesity related traits(Liu et al., 2022). Moreover, recent evidence suggested that in failing hearts the most robust alteration is the upregulation of distinct PE species and that the pressure-induced cardiac PE induction results in a decreased PC/PE ratio (Salatzki et al., 2018). Interestingly, our overall CVD population presented with reduced PC/PE ratio in plasma while NLRP3 plasma levels increased. It is well accepted that a spectrum of diseases characterized by chronic low-grade inflammation as obesity-related disorders, like IR, referred to NLRP3 inflammasome, but in our study we show for the first time the inverse association between NLRP3 circulating levels and decreased PC/PE plasma ratio in a CVD population with IR risk (Warmbrunn et al., 2021). Normally PC is mostly present on the outer cell membrane, whereas PE is usually located within the inner cell membrane. The disruption of PC and PE distribution on cell membranes leads to alterations on its permeability potential (Meikle and Summers, 2017) in addition to being positively associated with Framingham score (Warmbrunn et al., 2021). Due to the impact of NLRP3 and PC/PE molar ratio on heart metabolism and inflammation we also investigated the potential involvement of phospholipids metabolites and the inflammasome in heart remodeling; and we found that the overweight CVD patients with IR risk presented a positive association between NLRP3 plasma levels and echocardiographic parameters used to describe LV chamber change, including relative wall thickness (RTW%), one of the two parameters used to categorize both cardiac remodeling and hypertrophy (Lang et al., 2015). Interestingly, in CVD patients who present both IR risk and left atrium enlargement, NLRP3 plasma levels resulted increased, suggesting that NLRP3 plasma level can be a potential signature of early diastolic dysfunction, although no statistically significant alterations were found between this target and echo doppler parameter (E/A). In contrast, our cohort with IR risk showed a decreased level of PC/PE molar ratio, in presence of LV remodeling and cardiac failure (reduced ejection fraction) suggesting the potential role of them in the clinical management of cardiac decline. Indeed, the major limitation of this study is the small number of patients enrolled that only allowed the investigation of few IR risk and LV remodeling categories, besides the lack of prospective data to better assess the dyslipidemia and IR-risk involvement in CVD complications. This study can be seen as an initial investigation to better understand the onset of cardiac remodeling associated to PC/PE-induced NLRP3 inflammasome in CVD patients

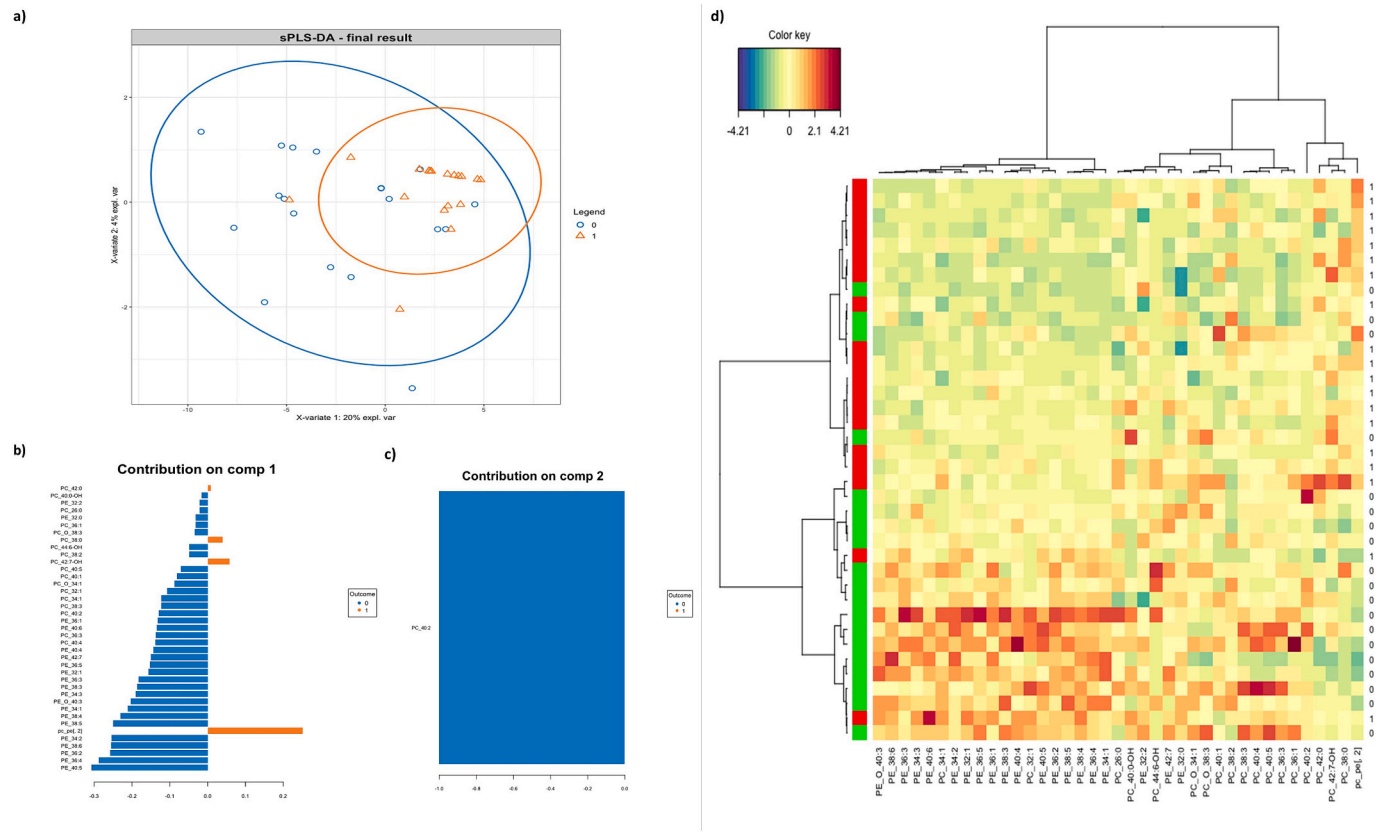

Fig. 4. sPLS-DA categorization of PC and PE species according to the median value of NLRP3. a) To study the influence of meta-inflammation expressed as the plasma mediator NLRP3, circulating species of PC and PE were categorized according to the median value of NLRP3 (1.48ng/ml). b) The 3-fold cross-validation method used 2 components with 39 and 1 features in PLS-DA classification. In the presence of high NLRP3 (>1.48ng/ml), PC and PE species were reduced (b) compared with overweight CVD patients with low NLRP3 (<1.48 ng/ml) (c). The selected variables were used to create a heatmap according to the median cut-off of NLRP3 (d). On the right side NLRP3 is represented categorized according to the median NLRP3 cut-off: green represents all NLRP3 values less than 1.48ng/ml and red all values greater than up to 1.48/ml. The heatmap shows the statistically significant trend of increasing circulating species of PC and PE in overweight CVD patients without risk of IR (0) and with low circulating levels of NLRP3 (green). In contrast, in the presence of IR risk (1) and high circulating plasma levels of NLRP3 (red), PC and PE species are reduced.

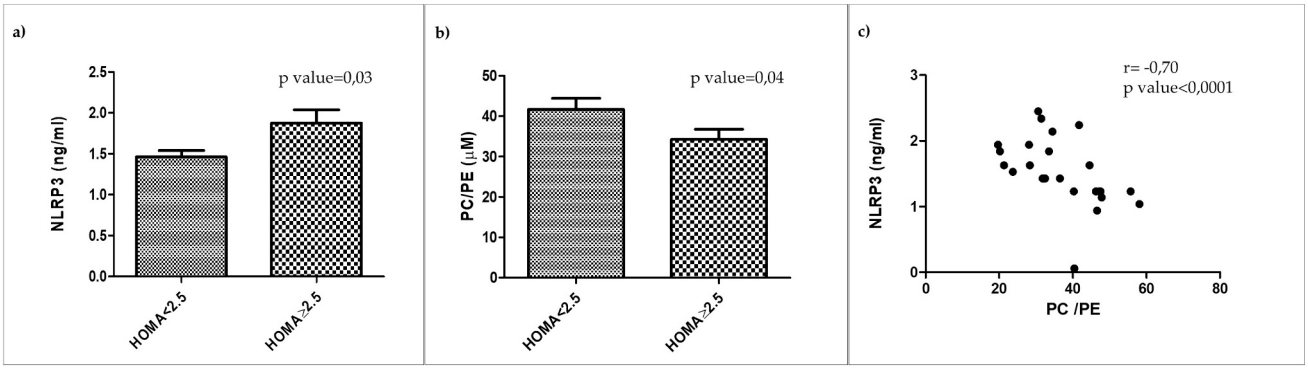

Fig. 5. CVD patients with IR risk presented a metabolic profile associated to LV remodeling. CVD patients with IR risk have higher levels of NLRP3 (a) and lower levels of PC/PE molar plasma ratio (b) than CVD without IR risk. CVD population presented an inverselly association between NLRP3 level and PC/PE molar ratio in plasma (c).

with IR risk. Further prospective studies should evaluate if the PC/PE ratio and NLRP3 inflammasome are indeed important for maladaptive LV remodeling onset and progression, to pave the way for new metabolic targets of early LV remodeling onset and progression toward CVD patients who present with IR risk.

5. Conclusion

Here we show that lipid perturbations occurring during meta-inflammation in overweight CVD populations is associated with LV maladaptive remodeling. This work highlights the PC and PE systemic impairment associated with IR risk with consequence in systemic inflammation and heart response. Our data highlight the direct association between NLRP3 inflammasome and PC/PE molar ratio in plasma

a)

NLRP3 association in overweight CVDs patients with IR risk		
Variables (y)	**R**	***p***
Diastolic blood pressure (mmHg)	0,57	0,003
End diastolic diameter (cm)	0,29	0,01
Relative wall thickness (%)	0,43	0,04
VTD/BSA	0,55	0,01

b)

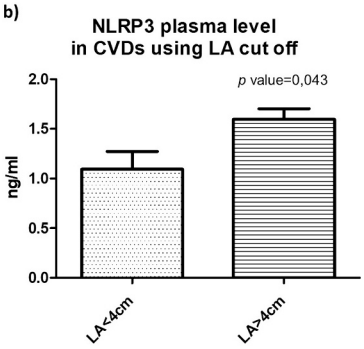

c)

PC/PE association in overweight CVDs patients with IR risk		
Variables (y)	**R**	***p***
Systolic blood pressure (mmHg)	-0,78	0,03
End diastolic diameter (cm)	-0,50	0,001
Relative wall thickness (%)	-0,46	0,04
LV diastolic volume/BSA (ml/m^2)	-0,47	0,01
LV systolic volume/BSA (ml/m^2)	0,44	0,02
EF (%)	-0,41	0,03

Fig. 6. Association between PC/PE ratio and NLRP3 plasma level and cardiac remodeling in overweight CVD patients with IR risk. Overweight CVD patients with IR risk (HOMA≥2,5) show a positive association between NLRP3 plasma level and cardiac parameter of LV remodeling, with a direct relations with diastolic blood pressure ($p < 0,003$, Spearman $R = 0,57$); end diastolic diameter ($p < 0,01$; Spearman R = 0,29); relative wall thickness ($p < 0,04$; Spearman R = 0,43); and VTD/BSA ($p < 0,01$; Spearman R = 0,55)(a). Overweight CVD patients with HOMA≥2,5 who present LA enlargement (LA > 4 cm) have also higher level of NLRP3 than patients without LA enlargement (1,09 ± 0,53 ng/ml vs 1,59 ± 0,45 ng/ml; $p < 0.04$), suggesting the potential association between NLRP3 circulating level and diastolic disfunction (b). In Overweight CVD patients with IR risk (HOMA<2) PC/PE ratio is reduced in presence of LV remodeling and cardiac failure due to the inverse association between their ratio and echocardiographic parameters including systolic blood pressure ($p < 0,03$; Spearman R = -0,78); end diastolic diameter ($p < 0.001$; Spearman R = -0,50); relative wall thickness ($p < 0,04$; Spearman R = -0,46); LV diastolic volume/BSA ($p < 0,01$; Spearman R = -0,47); LV systolic volume /BSA ($p < 0,02$; Spearman R = -0,44); EF($p < 0,03$; Spearman R = -0,41) (c).

suggesting their involvement in maladaptive heart responses. Indeed, CVD patients with IR risk presented a reduction in PC/PE molar ratio associated with NLRP3 activation in plasma, thus losing their systemic protection and predisposing them to LV geometry changes.

Institutional review board statement

The study was conducted in accordance with the Declaration of Helsinki and approved by the Ethics Committee of ASL Milano Due (No. 2516) for studies involving humans.

Informed consent statement

Informed consent was obtained from people involved in the study. We understood patients provided written informed consent for both the experiment and the publication.

Funding

The publication fee has been supported by Ricerca Corrente from Italian Ministry of Health - The project has been supported by the "Fondazione Romeo ed Erica Invernizzi" (Italy), by the Exceles LX22NPO5104 (given by the Ministry of Education, Youth and Sport of the Czech Republic), MH CZ DRO VFN 64165 (given by the Czech Ministry of Health) and Cooperatio Medical Diagnostics (Charles University project).

CRediT authorship contribution statement

Elena Vianello: Conceptualization, Data curation, Investigation, Project administration, Formal analysis, Writing – original draft. **Federico Ambrogi:** Data curation, Formal analysis, Methodology, Software. **Marta Kalousová:** Supervision, Validation, Writing – review & editing. **Julietta Badalyan:** Data curation, Formal analysis, Software. **Elena Dozio:** Methodology, Supervision. **Lorenza Tacchini:** Validation, Visualization. **Gerd Schmitz:** Methodology, Investigation. **Tomáš Zima:** Supervision, Funding acquisition. **Gregory J. Tsongalis:** Validation, Supervision, Writing – review & editing. **Massimiliano M. Corsi-Romanelli:** Funding acquisition, Supervision, Validation.

Declaration of competing interest

The authors declare that there are no conflicts of interest.

Data availability

Data are available on request from the corresponding author: Elena Vianello elena.vianello@unimi.it

Acknowledgments

Authors thank the IRCCS Policlinico San Donato of Milan for patient's enrollment and tissues recovery.

References

Agarwal, M., Khan, S., 2020. Plasma lipids as biomarkers for Alzheimer's disease: a systematic review. Cureus 12, e12008.

Baumgartner, H. Chair, Hung, J. Co-Chair, Bermejo, J., Chambers, J.B., Edvardsen, T., Goldstein, S., Lancellotti, P., LeFevre, M., Miller Jr., F., Otto, C.M., 2017. Recommendations on the echocardiographic assessment of aortic valve stenosis: a focused update from the European Association of Cardiovascular Imaging and the American Society of Echocardiography. Eur. Heart J. Cardiovasc. Imaging 18, 254–275.

Bergland, A.K., Proitsi, P., Kirsebom, B.E., Soennesyn, H., Hye, A., Larsen, A.I., Xu, J., Legido-Quigley, C., Rajendran, L., Fladby, T., Aarsland, D., 2020. Exploration of plasma lipids in mild cognitive impairment due to Alzheimer's disease. J. Alzheimers Dis. 77, 1117–1127.

Bligh, E.G., Dyer, W.J., 1959. A rapid method of total lipid extraction and purification. Can. J. Biochem. Physiol. 37, 911–917.

Carvalho, L.S.F., Chaves-Filho, A.B., Yoshinaga, M.Y., 2022. Orchestrating a ceramide-phosphatidylcholine cardiovascular risk score: it ain't over 'til the fat layer sings. Eur. J. Prev. Cardiol. 29, 892–894.

Chaurasia, B., Summers, S.A., 2018. Ceramides - lipotoxic inducers of metabolic disorders: (trends in endocrinology and metabolism 26, 538-550; 2015). Trends Endocrinol. Metab. 29, 66–67.

Chaurasia, B., Summers, S.A., 2021. Ceramides in metabolism: key lipotoxic players. Annu. Rev. Physiol. 83, 303–330.

Chaurasia, B., Ying, L., Talbot, C.L., Maschek, J.A., Cox, J., Schuchman, E.H., Hirabayashi, Y., Holland, W.L., Summers, S.A., 2021. Ceramides are necessary and sufficient for diet-induced impairment of thermogenic adipocytes. Mol. Metab. 45, 101145.

Dominic, A., Le, N.T., Takahashi, M., 2022. Loop between NLRP3 inflammasome and reactive oxygen species. Antioxid. Redox Signal. 36, 784–796.

D'Souza, K., Nzirorera, C., Kienesberger, P.C., 2016. Lipid metabolism and signaling in cardiac lipotoxicity. Biochim. Biophys. Acta 1861, 1513–1524.

Engin, A., 2017a. Fat cell and fatty acid turnover in obesity. Adv. Exp. Med. Biol. 960, 135–160.

Engin, A.B., 2017b. What is lipotoxicity? Adv. Exp. Med. Biol. 960, 197–220.

Fernandez, C., Sandin, M., Sampaio, J.L., Almgren, P., Narkiewicz, K., Hoffmann, M., Hedner, T., Wahlstrand, B., Simons, K., Shevchenko, A., James, P., Melander, O., 2013. Plasma lipid composition and risk of developing cardiovascular disease. PLoS One 8, e71846.

Frostegard, J., 2022. Antibodies against phosphorylcholine and protection against atherosclerosis, cardiovascular disease and chronic inflammation. Expert Rev. Clin. Immunol. 18, 525–532.

Gaggini, M., Carli, F., Rosso, C., Younes, R., D'Aurizio, R., Bugianesi, E., Gastaldelli, A., 2019. Altered metabolic profile and adipocyte insulin resistance mark severe liver fibrosis in patients with chronic liver disease. Int. J. Mol. Sci. 20.

Gong, J., Campos, H., McGarvey, S., Wu, Z., Goldberg, R., Baylin, A., 2011. Adipose tissue palmitoleic acid and obesity in humans: does it behave as a lipokine? Am. J. Clin. Nutr. 93, 186–191.

Grebe, A., Hoss, F., Latz, E., 2018. NLRP3 inflammasome and the IL-1 pathway in atherosclerosis. Circ. Res. 122, 1722–1740.

Guilherme, A., Rowland, L.A., Wang, H., Czech, M.P., 2023. The adipocyte supersystem of insulin and cAMP signaling. Trends Cell Biol. 33, 340–354.

Hellberg, S., Silvola, J.M., Kiugel, M., Liljenback, H., Metsala, O., Viljanen, T., Metso, J., Jauhiainen, M., Saukko, P., Nuutila, P., Yla-Herttuala, S., Knuuti, J., Roivainen, A., Saraste, A., 2016. Type 2 diabetes enhances arterial uptake of choline in atherosclerotic mice: an imaging study with positron emission tomography tracer (1)(8)F-fluoromethylcholine. Cardiovasc. Diabetol. 15, 26.

Higashikuni, Y., Liu, W., Numata, G., Tanaka, K., Fukuda, D., Tanaka, Y., Hirata, Y., Imamura, T., Takimoto, E., Komuro, I., Sata, M., 2023. NLRP3 inflammasome activation through heart-brain interaction initiates cardiac inflammation and hypertrophy during pressure overload. Circulation 147, 338–355.

Hornemann, T., 2022. Lipidomics in biomarker research. Handb. Exp. Pharmacol. 270, 493–510.

Jaiswal, M., Schinske, A., Pop-Busui, R., 2014. Lipids and lipid management in diabetes. Best Pract. Res. Clin. Endocrinol. Metab. 28, 325–338.

Kane, J.P., Pullinger, C.R., Goldfine, I.D., Malloy, M.J., 2021. Dyslipidemia and diabetes mellitus: role of lipoprotein species and interrelated pathways of lipid metabolism in diabetes mellitus. Curr. Opin. Pharmacol. 61, 21–27.

Kao, Y.C., Ho, P.C., Tu, Y.K., Jou, I.M., Tsai, K.J., 2020. Lipids and Alzheimer's disease. Int. J. Mol. Sci. 21.

Kelley, N., Jeltema, D., Duan, Y., He, Y., 2019. The NLRP3 inflammasome: an overview of mechanisms of activation and regulation. Int. J. Mol. Sci. 20 (13), 3328.

Kennedy, E.P., 1957. Metabolism of lipides. Annu. Rev. Biochem. 26, 119–148.

Kumar, A., Sundaram, K., Mu, J., Dryden, G.W., Sriwastva, M.K., Lei, C., Zhang, L., Qiu, X., Xu, F., Yan, J., Zhang, X., Park, J.W., Merchant, M.L., Bohler, H.C.L., Wang, B., Zhang, S., Qin, C., Xu, Z., Han, X., McClain, C.J., Teng, Y., Zhang, H.G., 2021. High-fat diet-induced upregulation of exosomal phosphatidylcholine contributes to insulin resistance. Nat. Commun. 12, 213.

Laitinen, I.E., Luoto, P., Nagren, K., Marjamaki, P.M., Silvola, J.M., Hellberg, S., Laine, V. J., Yla-Herttuala, S., Knuuti, J., Roivainen, A., 2010. Uptake of 11C-choline in mouse atherosclerotic plaques. J. Nucl. Med. 51, 798–802.

Lang, R.M., Badano, L.P., Mor-Avi, V., Afilalo, J., Armstrong, A., Ernande, L., Flachskampf, F.A., Foster, E., Goldstein, S.A., Kuznetsova, T., Lancellotti, P., Muraru, D., Picard, M.H., Rietzschel, E.R., Rudski, L., Spencer, K.T., Tsang, W., Voigt, J.U., 2015. Recommendations for cardiac chamber quantification by echocardiography in adults: an update from the American Society of Echocardiography and the European Association of Cardiovascular Imaging. J. Am. Soc. Echocardiogr. 28, 1–39 e14.

Le Cao, K.A., Boitard, S., Besse, P., 2011. Sparse PLS discriminant analysis: biologically relevant feature selection and graphical displays for multiclass problems. BMC Bioinformatics 12, 253.

Li, C., Guo, S., Pang, W., Zhao, Z., 2020. Crosstalk between acid sphingomyelinase and inflammasome signaling and their emerging roles in tissue injury and fibrosis. Front. Cell Dev. Biol. 7, 378.

Liu, J., de Vries, P.S., Del Greco, M.F., Johansson, A., Schraut, K.E., Hayward, C., van Dijk, K.W., Franco, O.H., Hicks, A.A., Vitart, V., Rudan, I., Campbell, H., Polasek, O., Pramstaller, P.P., Wilson, J.F., Gyllensten, U., van Duijn, C.M., Dehghan, A., Demirkan, A., 2022. A multi-omics study of circulating phospholipid markers of blood pressure. Sci. Rep. 12, 574.

Meikle, P.J., Summers, S.A., 2017. Sphingolipids and phospholipids in insulin resistance and related metabolic disorders. Nat. Rev. Endocrinol. 13, 79–91.

Michos, E.D., McEvoy, J.W., Blumenthal, R.S., 2019. Lipid management for the prevention of atherosclerotic cardiovascular disease. N. Engl. J. Med. 381, 1557–1567.

Mridha, A.R., Wree, A., Robertson, A.A.B., Yeh, M.M., Johnson, C.D., Van Rooyen, D.M., Haczeyni, F., Teoh, N.C., Savard, C., Ioannou, G.N., Masters, S.L., Schroder, K., Cooper, M.A., Feldstein, A.E., Farrell, G.C., 2017. NLRP3 inflammasome blockade reduces liver inflammation and fibrosis in experimental NASH in mice. J. Hepatol. 66, 1037–1046.

Murakami, M., 2011. Lipid mediators in life science. Exp. Anim. 60, 7–20.

Obesity: preventing and managing the global epidemic. Report of a WHO consultation, 2000. World Health Organ. Tech. Rep. Ser. 894 (i-xii), 1–253.

Qiu, Z., He, Y., Ming, H., Lei, S., Leng, Y., Xia, Z.Y., 2019. Lipopolysaccharide (LPS) aggravates high glucose- and hypoxia/reoxygenation-induced injury through activating ROS-dependent NLRP3 inflammasome-mediated pyroptosis in H9C2 cardiomyocytes. J. Diabetes Res. 8151836.

Quintana, F.J., Yeste, A., Weiner, H.L., Covacu, R., 2012. Lipids and lipid-reactive antibodies as biomarkers for multiple sclerosis. J. Neuroimmunol. 248, 53–57.

Rayner, J.J., Banerjee, R., Holloway, C.J., Lewis, A.J.M., Peterzan, M.A., Francis, J.M., Neubauer, S., Rider, O.J., 2018. The relative contribution of metabolic and structural abnormalities to diastolic dysfunction in obesity. Int. J. Obes. 42, 441–447.

Rivas Serna, I.M., Sitina, M., Stokin, G.B., Medina-Inojosa, J.R., Lopez-Jimenez, F., Gonzalez-Rivas, J.P., Vinciguerra, M., 2021. Lipidomic profiling identifies signatures of poor cardiovascular health. Metabolites 11.

Rohart, F., Gautier, B., Singh, A., Le Cao, K.A., 2017. mixOmics: an R package for omics feature selection and multiple data integration. PLoS Comput. Biol. 13 (11), e1005752.

Roppongi, M., Izumisawa, M., Terasaki, K., Muraki, Y., Shozushima, M., 2019. (18)F-FDG and (11)C-choline uptake in proliferating tumor cells is dependent on the cell cycle in vitro. Ann. Nucl. Med. 33, 237–243.

Salatzki, J., Foryst-Ludwig, A., Bentele, K., Blumrich, A., Smeir, E., Ban, Z., Brix, S., Grune, J., Beyhoff, N., Klopfleisch, R., Dunst, S., Surma, M.A., Klose, C., Rothe, M., Heinzel, F.R., Krannich, A., Kershaw, E.E., Beule, D., Schulze, P.C., Marx, N., Kintscher, U., 2018. Adipose tissue ATGL modifies the cardiac lipidome in pressure-overload-induced left ventricular failure. PLoS Genet. 14, e1007171.

Sanchez-Lopez, E., Zhong, Z., Stubelius, A., Sweeney, S.R., Booshehri, L.M., Antonucci, L., Liu-Bryan, R., Lodi, A., Terkeltaub, R., Lacal, J.C., Murphy, A.N., Hoffman, H.M., Tiziani, S., Guma, M., Karin, M., 2019. Choline uptake and metabolism modulate macrophage IL-1beta and IL-18 production. Cell Metab. 29, 1350–1362 e7.

Scheja, L., Heeren, J., 2019. The endocrine function of adipose tissues in health and cardiometabolic disease. Nat. Rev. Endocrinol. 15, 507–524.

Seki, M., Kawai, Y., Ishii, C., Yamanaka, T., Odawara, M., Inazu, M., 2017. Functional analysis of choline transporters in rheumatoid arthritis synovial fibroblasts. Mod. Rheumatol. 27, 995–1003.

Shalaurova, I., Connelly, M.A., Garvey, W.T., Otvos, J.D., 2014. Lipoprotein insulin resistance index: a lipoprotein particle-derived measure of insulin resistance. Metab. Syndr. Relat. Disord. 12, 422–429.

Snider, S.A., Margison, K.D., Ghorbani, P., LeBlond, N.D., O'Dwyer, C., Nunes, J.R.C., Nguyen, T., Xu, H., Bennett, S.A.L., Fullerton, M.D., 2018. Choline transport links macrophage phospholipid metabolism and inflammation. J. Biol. Chem. 293, 11600–11611.

Sokolova, M., Yang, K., Hansen, S.H., Louwe, M.C., Kummen, M., Hov, J.E.R., Sjaastad, I., Berge, R.K., Halvorsen, B., Aukrust, P., Yndestad, A., Ranheim, T., 2020. NLRP3 inflammasome deficiency attenuates metabolic disturbances involving alterations in the gut microbial profile in mice exposed to high fat diet. Sci. Rep. 10, 21006.

Sondergaard, E., Espinosa De Ycaza, A.E., Morgan-Bathke, M., Jensen, M.D., 2017. How to measure adipose tissue insulin sensitivity. J. Clin. Endocrinol. Metab. 102, 1193–1199.

Suceveanu, A.I., Mazilu, L., Katsiki, N., Parepa, I., Voinea, F., Pantea-Stoian, A., Rizzo, M., Botea, F., Herlea, V., Serban, D., Suceveanu, A.P., 2020. NLRP3 inflammasome biomarker-could be the new tool for improved cardiometabolic syndrome outcome. Metabolites 10.

van der Veen, J.N., Kennelly, J.P., Wan, S., Vance, J.E., Vance, D.E., Jacobs, R.L., 2017. The critical role of phosphatidylcholine and phosphatidylethanolamine metabolism in health and disease. Biochim. Biophys. Acta Biomembr. 1859 (9 Part B), 1558–1572.

van Meer, G., 2005. Cellular lipidomics. EMBO J. 24, 3159–3165.

Vandanmagsar, B., Youm, Y.H., Ravussin, A., Galgani, J.E., Stadler, K., Mynatt, R.L., Ravussin, E., Stephens, J.M., Dixit, V.D., 2011. The NLRP3 inflammasome instigates obesity-induced inflammation and insulin resistance. Nat. Med. 17, 179–188.

Visseren, F.L.J., Mach, F., Smulders, Y.M., Carballo, D., Koskinas, K.C., Back, M., Benetos, A., Biffi, A., Boavida, J.M., Capodanno, D., Cosyns, B., Crawford, C., Davos, C.H., Desormais, I., Angelantonio, E.D., Franco, O.H., Halvorsen, S., Hobbs, F. D. Richard, Hollander, M., Jankowska, E.A., Michal, M., Sacco, S., Sattar, N., Tokgozoglu, L., Tonstad, S., Tsioufis, K.P., van Dis, I., van Gelder, I.C., Wanner, C., Williams, B., E. S. C. Scientific Document Group, 2022. 2021 ESC guidelines on cardiovascular disease prevention in clinical practice: developed by the task force for cardiovascular disease prevention in clinical practice with representatives of the European Society of Cardiology and 12 medical societies with the special contribution of the European Association of Preventive Cardiology (EAPC). Rev. Esp. Cardiol. (Engl. Ed.) 75, 429.

Wallace, M., Morris, C., O'Grada, C.M., Ryan, M., Dillon, E.T., Coleman, E., Gibney, E.R., Gibney, M.J., Roche, H.M., Brennan, L., 2014. Relationship between the lipidome, inflammatory markers and insulin resistance. Mol. BioSyst. 10 (6), 1586–1595.

Warmbrunn, M.V., Koopen, A.M., de Clercq, N.C., de Groot, P.F., Kootte, R.S., Bouter, K. E.C., Ter Horst, K.W., Hartstra, A.V., Serlie, M.J., Ackermans, M.T., Soeters, M.R., van Raalte, D.H., Davids, M., Nieuwdorp, M., Groen, A.K., 2021. Metabolite profile of treatment-naive metabolic syndrome subjects in relation to cardiovascular disease risk. Metabolites 11.

Wasserman, A.H., Venkatesan, M., Aguirre, A., 2020. Bioactive lipid signaling in cardiovascular disease, development, and regeneration. Cells 9.

Wiesner, P., Leidl, K., Boettcher, A., Schmitz, G., Liebisch, G., 2009. Lipid profiling of FPLC-separated lipoprotein fractions by electrospray ionization tandem mass spectrometry. J. Lipid Res. 50, 574–585.

Xie, H., Yang, X., Cao, Y., Long, X., Shang, H., Jia, Z., 2022. Role of lipoic acid in multiple sclerosis. CNS Neurosci. Ther. 28, 319–331.

Zhan, X., Li, Q., Xu, G., Xiao, X., Bai, Z., 2022. The mechanism of NLRP3 inflammasome activation and its pharmacological inhibitors. Front. Immunol. 13, 1109938.